SME Annual Meeting
Feb. 27 - Mar. 02, 2022, Salt Lake City, UT

Preprint 22-050

OPTIMIZATION OF AUXILIARY FAN PLACEMENT FOR LARGE-OPENING UNDERGROUND STONE MINES

E. Watkins, CDC NIOSH, Pittsburgh, PA
V. Gangrade, CDC NIOSH, Pittsburgh, PA

Large-opening stone mines often rely on natural ventilation and a network of auxiliary fans to produce adequate ventilation conditions in the mine instead of main mine fans, which are commonly utilized in coal mines. Large air volumes in underground stone mines, poor ventilation practices, and low operating budgets for mine ventilation potentially increase mine workers' risk for dust, silica, and diesel particulate matter (DPM) emissions exposure. To help improve mine ventilation practices, the optimal auxiliary fan location for maximum airflow production from a ventilated intersection was determined using a combination of field measurements and computational fluid dynamics (CFD) modeling. In this study, conducted by researchers at the National Institute for Occupational Safety and Health (NIOSH), airflow quantity and fan data were collected at a partner mine to be applied as CFD model input parameters and comparison data for model validation. A six-foot diameter auxiliary propeller fan was introduced into the validated CFD model at three locations at a mine entry intersection with established ventilation flow perpendicular to the fan direction. Placing the fan on the opposite side of the intersection from the target active face area produced the highest ventilation flow rates at the downstream locations tested and produced the lowest amount of air re-circulation. The findings show that optimizing the placement of an auxiliary fan may increase the net effective ventilation flow rate by 70,000 cfm and reduce recirculation by 26%, which maximizes the potential effectiveness of large-opening stone mine ventilation systems and decreases mine worker exposures to airborne contaminants.

INTRODUCTION

Historically, a majority of limestone mining has been conducted through surface mining operations with NIOSH reporting that out of the 4,362 crushed stone mines in operation, only 111 were underground mines (NIOSH, 2015). Over the last two decades, the number of surface operations has been decreasing while the number of underground mines is gradually increasing. In addition, the existing underground mines are moving towards greater depths and multiple levels. The increasing trend of underground mining is exposing the industry to greater health and safety risks. Underground stone mines come with a unique set of challenges, of which ventilation is often the primary challenge. Ventilation of these mines is challenging because of the large entry sizes leading to low airflow velocities and increased natural ventilation effects. Presently, the continuing and emerging air quality issues in large-opening mines include silica dust, diesel particulate matter (DPM), noxious gases (from diesel equipment, welding, and production blasts), and the lack of visibility due to fog. Contaminants can be reduced through proper ventilation methods and by utilizing preventative measures such as installing new engines and novel filters. Effective ventilation in these mines generally requires a combination of delivering needed air quantities and effective planning and placement of ventilation control devices such as auxiliary fans and stoppings (Grau and Krog 2009).

Large-opening stone mine ventilation systems are unique compared to underground coal mines. Coal mine ventilation is characterized by lower air quantities but much higher resistances, while large-opening stone mines distribute high ventilation quantities but with low resistance. The ventilation systems vary between stone operations as well, with large variations in numbers of entries, depths of operations, slopes of deposit, use of benching, and use of natural ventilation. The mining safety and health literature is replete with coal mine ventilation research from around the world. In comparison to the volume of coal mine ventilation studies, less research has been done to study and improve the ventilation of large-opening stone mines.

During the 2000s, NIOSH conducted extensive research to study large-opening mine ventilation. The research suggested that these mines face three primary ventilation challenges: moving adequate volumes of ventilation air, controlling and directing the airflow, and planning ventilation systems that work well with production requirements (Grau et al. 2006). Multiple studies were also conducted that showed increased suitability of propeller fans for low resistance ventilation systems present in stone mines compared to the vane axial fans commonly applied in coal mines (Grau et al. 2004; Krog and Grau 2006). Studies on the effectiveness of different large-opening stone mine ventilation stoppings showed steel stoppings were effective for permanent stopping locations, fabric stoppings were more effective closer to blasting areas, and a long stone pillar could perform the same role as a row of stoppings (Grau et al. 2002; Krog and Grau 2008). A recent study by Pennsylvania State University researchers tracked natural ventilation parameters in a large-opening underground stone mine to assess the impact of atmospheric conditions on the mine ventilation systems (Gendrue et al. 2021). Despite the previous research into large-opening stone mine ventilation systems, there has been little application of computational fluid dynamics (CFD) models on these ventilation systems.

Even though CFD modeling software programs, whether commercially available or open source, have been widely utilized by research institutions and universities to solve mining ventilation issues, the application of such models is relatively new with regards to large-opening stone mine ventilation issues. In South Korea, a study utilized Ansys Fluent software to compare the economic feasibility and ventilation potential for a high-pressure against a low-pressure auxiliary fan, using a combination of field work and CFD modeling (Lee and Nguyen 2015). Ansys Fluent, the software package chosen for this study, is often chosen for its user-friendly graphical user interface, integrated geometry/meshing tools, and the ability to solve a wide range of flow regimes. For all flow modeling in Fluent, the equations for conservation of mass and momentum are solved with additional equations solved for energy, species transport, and turbulence if required (ANSYS 2014). This paper details the findings from a series of Ansys Fluent models that estimated the induced ventilation from a booster fan placed at three locations within a large-opening stone mine intersection that has established ventilation flow perpendicular to the fan direction.

CFD MODEL SETUP

Analysis on the effects of fan placement on induced ventilation flow was conducted with the computational fluid dynamics (CFD) software Ansys Fluent. The CFD model used in this study consisted of the lower section of an underground large-opening stone mine, which utilized one intake slope, one haulage entrance slope, and two exhausting slopes for ventilation and transportation of equipment to the section. Figure 1 details the standard layout of the mine geometry and fan locations incorporated into the CFD model. Four propeller booster fans are implemented by the mine to produce approximately 385,000 cubic feet per minute (cfm) of flow down the intake slope and direct air to the active faces on the section. The diameters of the booster fans are 12 feet (ft) for Fan 1, 10 ft for Fan 2, and 6 ft for Fans 3 and 4. The

average dimensions on the mine entries are 45 ft by 20 ft with 16 ft in additional height in a benched area adjacent to booster Fan 3.

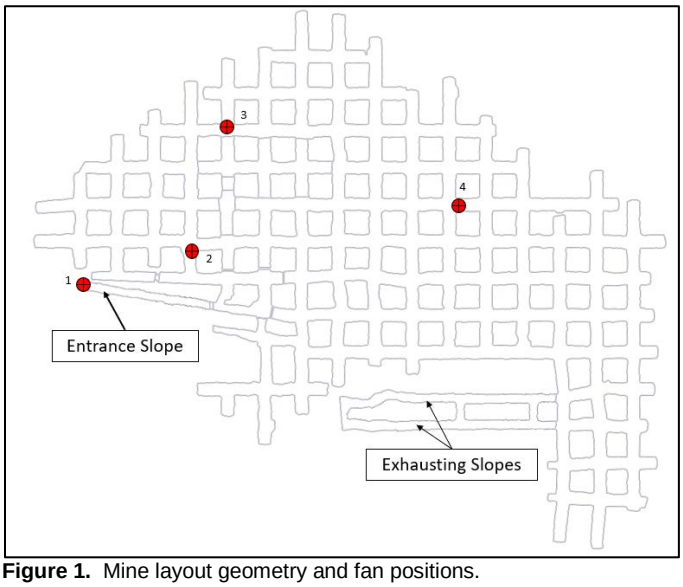

Figure 1. Mine layout geometry and fan positions.

The CFD model uses a combination of pressure inlets, pressure outlets, and internal fan boundary conditions to replicate the ventilation flow in the mine. Fan 1 induced flow is represented by the pressure inlet since it is located out of the bounds of the model geometry but still crucial to the ventilation design. The main outlet in the model is represented by a pressure outlet where the two exhausting slopes connect to one entry. Fans 2, 3, and 4 use the internal fan boundary conditions to model the pressure-flowrate relationship of the fans. The fan boundary conditions were located at the center of fan casings that were the same inner diameter of each respective fan, with a casing thickness of 6 inches. The wall boundary layers in the model have a wall roughness of approximately 10 inches and the standard k-epsilon turbulence model was utilized. The k-epsilon turbulence model is a commonly utilized Reynolds-averaged Navier Stokes (RANS) model which governs transport based on averaged flow quantities to reduce computational demand.

The model mesh consisted of polyhedral elements meshed to faces with 3 wall inflation layers, 6 cells per gap, and a curvature capture angle of 10 degrees. To ensure that the mesh is independent, the pressure jump induced flowrates of Fans 2 and 4 were tracked as the model was repeatedly run with a refined mesh until the values remained unchanged with further mesh refinement.

The partner mine performed a series of traverses and point measurements for airflow velocity across 16 locations throughout the mine to assess the CFD model validity compared to the actual mine ventilation conditions. The locations of comparison consisted of taking measurements in entries near the air intake slope, entries adjacent to Fan 2, entries surrounding Fan 4 and locations of high curtain leakage. The percent difference between the field and modeled air flow rates ranged between a 0.4% to 36.4% difference with an average of 13.2%. The model flowrates had the largest deviation from the mine data in the entries closest to Fan 2. This is most likely due to not having an exact pillar geometry and fan placement for where the Fan 2 outflow is split by the corner of the pillar opposite of the fan. The split flow creates a highly turbulent flow region and the airflow quantities on each side of the pillar are highly dependent on the pillar geometry and fan position. Given potential sources of human error during the data collection process and a difficulty to traverse the entry in its entirety, the difference between the field and model measurements in conjunction with the correct airflow directions were considered sufficient to determine that the CFD model methodology of using internal fan pressure boundary conditions could be utilized to test the fan placement of Fan 3. Figure 2 shows a contour of velocity for the CFD model representing the baseline mine ventilation conditions needed to test fan placement with Fan 3 turned off.

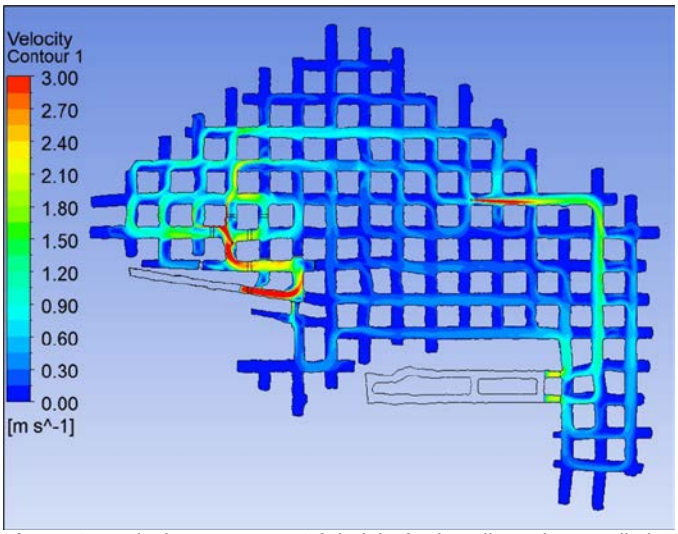

Figure 2. Velocity contour at 6-ft height for baseline mine ventilation model.

FAN PLACEMENT TEST DESIGN

The effects of varying placement of Fan 3 within a ventilated intersection was modeled with the fan tested at three locations to maximize effective flowrate and reduce recirculation. The direction of Fan 2 was perpendicular to the established ventilation flow to provide airflow to two potential active face zones downstream of the fan. The three fan locations were in the center of the intersection, on the opposite side of the intersection from the face zones and on the same side of the intersection as the face zones. Figure 3 displays the locations of the three fan placements, the face zones, and the evaluation points with their directional vectors used to compare the airflows induced by the different fan locations.

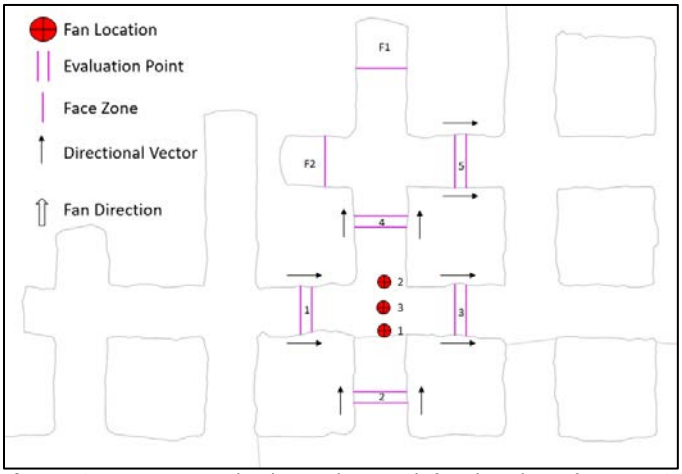

Figure 3. Layout evaluation points and fan locations for Fan 3 placement tests.

The fan locations were compared based on the total flowrate and the net flowrate at each of the five evaluation points, the two face zones, and the fan internal boundary surface. The total flowrate is calculated by taking the integral of the absolute velocity scalar of the control surface that represents each of the evaluation points. The net flowrate is calculated by the velocity integral of the control surface for either the u or v directional velocity vectors as shown in Figure 3. The total flowrate measure provides an indicator for the quantity of ventilation flow at that point, and the net flowrate measure provides an indicator for the effective quantity of ventilation flow that will also ventilate downstream of that point. The difference between the total

and net flowrates provides an estimate of airflow that is caused by recirculation across the control surface. A measure for percent of airflow that represents recirculation is then assessed by dividing the recirculation airflow amount by the total airflow.

FAN PLACEMENT TEST RESULTS

As described previously, the three fan locations were evaluated based on total flowrate, net flowrate, and recirculation at evaluation points, face zones, and the fan surface. Table 1 displays the total flowrate, Table 2 displays the net flowrate, and Table 3 shows the percent recirculation for each fan and evaluation location. The net flow is the same as the total flow at the face and fan locations, so the values for those locations are only shown in Table 1.

Table 1. Total Flowrate (kcfm).

Evaluation Location	Fan Location		
	1	2	3
EP 1	149.74	190.15	166.44
EP 2	102.05	98.89	63.31
EP 3	56.74	154.17	108.95
EP 4	271.41	299.23	299.72
EP 5	151.82	124.76	107.66
Face 1	23.27	34.01	25.13
Face 2	32.95	56.96	54.73
Fan 3	62.21	59.88	60.39

Table 2. Net Flowrate (kcfm).

Evaluation Location	Fan Location		
	1	2	3
EP 1	143.79	179.85	159.11
EP 2	6.48	2.01	-24.81
EP 3	52.74	153.60	95.33
EP 4	97.55	28.31	38.88
EP 5	97.64	28.27	38.90

Table 3. Air Recirculation (%).

Evaluation Location	Fan Location		
	1	2	3
EP 1	3.98	5.42	4.40
EP 2	93.65	97.96	60.81
EP 3	7.06	0.37	12.50
EP 4	64.06	90.54	87.03
EP 5	35.69	77.34	63.87

At the evaluation point 4 (EP 4), which is the closet evaluation point downstream of the fans, fan locations 2 and 3 had the highest total flowrates as shown in Table 1. At the second point downstream of the fans, EP 5, fan location 1 produced the highest total flowrate, which clears air away from the face zones. Fan location 2 produced the highest total flowrates at both face zones 1 and 2, with fan location 1 producing the lowest for both. Fan location 1 measured the lowest flowrate at the ventilated intersection outflow, EP 3, which indicates that it entrained the most air from the airway. Fan location 1 also produced the highest flowrate of 62.2 kcfm, but each of the fan locations produced similar flowrates within 3 kcfm of each other.

Table 2 shows that fan location 1 produces the highest net flowrates at the two locations downstream of the fans, EP 4 and 5, which is representative of the ventilation flow that effectively clears out contaminants from the intersection adjacent to the active faces. Fan location 1 has a higher effective ventilation flow of almost 70 kcfm compared to location 2 and 60 kcfm compared to location 3, at EP locations 4 and 5. This is supported by the lower net flowrate at EP 3 for fan location 1, which indicates the amount of airflow that passes by the fan and does not get directed towards the active faces. Since the net flowrates are a directional value, the negative flowrate at EP 2 for fan location 3 indicated a net flowrate away from Fan 3 and the active face zones.

Fan location 1 measuring the lowest total flowrate of the fan locations but the highest net flowrate for the EP 4, suggests that the other fan locations produced large amounts of air recirculation. This result is supported by the higher percentages of air circulation for fan locations 2 and 3 at EP 4 for Table 3. Fan location 1 had a lower air recirculation percentage by roughly 26% compared to location 2 and 23% compared to location 3 at EP 4. At EP 5, fan location 1 had a lower recirculation percentage by almost 32% and 28% compared to the two other fan locations, respectively. The amount of air recirculation stayed mostly unchanged based on fan location for EP 1 and EP 3. The recirculation percentages at EP 4 and EP 5 are visualized with velocity contours as shown in Figure 4.

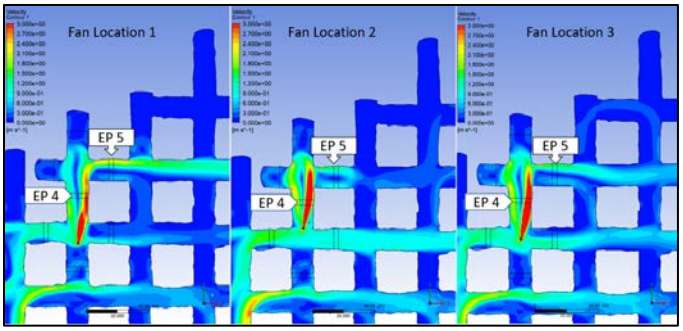

Figure 4. Velocity contours for each fan location at a height of 6 ft.

The increase in recirculation for fan locations 2 and 3 can be seen by the higher velocities in Figure 4 at the left side of EP 4 and the lower half of EP 5, which indicate higher airflows traveling back towards the location of the fans. The red contours in Figure 4, which represent the main air stream produced by the fans, shows the influence on how the distance traveled by the fan air stream through the ventilated intersection affects how close to the right of the entry the fan flow travels. The closer to the right side of the entry the fan flow is, the higher net flow that can be directed towards EP 5.

CONCLUSION

This study utilizes a combination of field ventilation data coupled with computational fluid dynamics modeling to test the effects of placing a six-foot-diameter propeller auxiliary fan at three positions within a ventilated intersection. The fan locations were compared based on total flowrate, net flowrate, and estimated percent air recirculation at various points upstream and downstream of the fans. Fan location 1 produced the highest net flowrate and lowest percentage of recirculation at the two downstream evaluation points but also produced the lowest flowrates at both fan locations modelled. Even though fan location 2 predicts the highest ventilation flowrates at both face locations, the high amount of recirculation, 77% to 90%, could result in higher levels of DPM and silica contaminants compared to the lower face ventilation flow shown by fan location 1.

The results determined from this study are meant to be utilized by mine personnel working in underground large-opening stone mines to determine the more efficient positions for their auxiliary propeller fan placement depending on their specific fan locations and other downstream key areas. Efficient fan placement maximizes air entrainment and net airflow, while minimizing air recirculation at key areas downstream of the fan location. Improving those parameters has the potential to reduce mine workers' exposure to airborne contaminants and improve the capabilities of the mine's ventilation network without the need to purchase additional equipment. However, additional analysis and testing is still required with DPM sources implemented into the model to fully understand the effects of net flowrate and percent air recirculation. The findings from this CFD modelling study still need to be verified through replicating the fan placement experiment in our partner mine to confirm any conclusions.

DISCLAIMER

The findings and conclusions in this report are those of the author(s) and do not necessarily represent the official position of the National Institute for Occupational Safety and Health, Centers for Disease Control and Prevention. Mention of any company or product does not constitute endorsement by NIOSH.

REFERENCES

1. ANSYS (2014). ANSYS Fluent Theory Guide. Release 15.0. Canonsburg, PA: SAS IP, Inc.

2. Gendrue, N., Liu, S., & Bhattacharyya, S. (2021). Field survey of mine ventilation system for large opening underground mines: Pressure, relative humidity, and temperature. Proceedings of the 18th North American Mine Ventilation Symposium, pp 489-497. DOI: 10.1201/9781003188476-50

3. Grau, R. H., Grau, R. H., Mucho, T. P., Mucho, T. P., Robertson, S. B., Robertson, Garcia, F. (2002). Practical techniques to improve the air quality in underground stone mines. Proceedings of the 9th North American Mine Ventilation Symposium, pp. 123–129. http://www.cdc.gov/niosh/mining/pubs/pubreference/outputid245.htm. Accessed March 2020

4. Grau, R. H., Robertson, S. B., Krog, R. B., Chekan, G. J., & Mucho, T. P. (2004). Raising the bar of ventilation for large-opening stone mines. Proceedings of the 10th North American Mine Ventilation Symposium, 349–355. Retrieved from https://www.cdc.gov/niosh/mining/UserFiles/works/pdfs/rbvlosm.pdf. Accessed March 2020.

5. Grau, R. H., Krog, R. B., & Robertson, S. B. (2006). Maximizing the ventilation of large-opening mines. Proceedings of the 11th North American Mine Ventilation Symposium 2006, 53–59. https://doi.org/10.1201/9781439833391.ch8

6. Grau, R. H., & Krog, R. (2009). Ventilating large opening mines. Journal of the Mine Ventilation Society of South Africa, 62(1), pp. 8–14.

7. Krog, R. B., & Grau, R. H. (2006). Fan selection for large-opening mines: vane-axial or propeller fans – which to choose? In 11th U.S./North American Mine Ventilation Symposium

8. Krog, R. B., & Grau, R. H. I. (2008). Using Mine Planning and Other Techniques to Improve Ventilation in Large-Opening Mines. SME Annual Meeting

9. Lee, C.W., & Nguyen, V. D. (2015). Development of a Low-Pressure Auxiliary Fan for Local Large-opening Limestone Mines. Tunnel & Underground Space Vol. 25, No. 6, 2015, pp. 543-555. http://dx.doi.org/10.7474/TUS.2015.25.6.543

10. NIOSH (2015). Mining Facts – 2015. Statistics: Stone Operators. Department of Health and Human Services (DHHS), Centers for Disease Control and Prevention (CDC), National Institute for Occupational Safety and Health (NIOSH)https://www.cdc.gov/niosh/mining/works/statistics/factsheets/miningfacts2015.html#StoneandSandGravelMineOperatorIndustrySector. Accessed August 2021.